Am J Transl Res 2022;14(6):3683-3697
www.ajtr.org /ISSN:1943-8141/AJTR0141701

Original Article

Inhibition of histone methyltransferase G9a effectively protected the kidney against ischemia-reperfusion injury

Peihsun Sung[1,2,3], Chihchao Yang[4], John Y Chiang[5,6], Chihhung Chen[7], Chiwen Luo[8,9], Honkan Yip[1,2,3,10,11,12]

[1]Division of Cardiology, Department of Internal Medicine, Kaohsiung Chang Gung Memorial Hospital and Chang Gung University College of Medicine, Kaohsiung, Taiwan; [2]Center for Shockwave Medicine and Tissue Engineering, Kaohsiung Chang Gung Memorial Hospital, Kaohsiung, Taiwan; [3]Institute for Translational Research in Biomedicine, Kaohsiung Chang Gung Memorial Hospital, Kaohsiung, Taiwan; [4]Division of Nephrology, Department of Internal Medicine, Kaohsiung Chang Gung Memorial Hospital and Chang Gung University College of Medicine, Kaohsiung, Taiwan; [5]Department of Computer Science and Engineering, National Sun Yat-Sen University, Kaohsiung, Taiwan; [6]Department of Healthcare Administration and Medical Informatics, Kaohsiung Medical University, Kaohsiung, Taiwan; [7]Divisions of General Medicine, Department of Internal Medicine, Kaohsiung Chang Gung Memorial Hospital and Chang Gung University College of Medicine, Kaohsiung, Taiwan; [8]Department of Surgery, Kaohsiung Medical University Hospital, Kaohsiung Medical University, Kaohsiung, Taiwan; [9]Division of Breast Oncology and Surgery, Department of Surgery, Kaohsiung Medical University Hospital, Kaohsiung Medical University, Kaohsiung, Taiwan; [10]School of Medicine, College of Medicine, Chang Gung University, Taoyuan, Taiwan; [11]Department of Medical Research, China Medical University Hospital, China Medical University, Taichung, Taiwan; [12]Department of Nursing, Asia University, Taichung, Taiwan

Received January 11, 2022; Accepted April 30, 2022; Epub June 15, 2022; Published June 30, 2022

Abstract: This study examined whether BIX01294, a histone methyltransferase G9a inhibitor, effectively preserves the renal function following acute kidney ischemia-reperfusion (AKIR) injury. Adult-male-SD rats (n = 24) were equally categorized into Group 1 (sham-operated control), Group 2 (AKIR + 1.0 cc N/S I.P. injection), and Group 3 (AKIR + BIX01294/5 mg/Kg by I.P. administration at 3 h after the procedure) and the kidneys were harvested at day-3 post-IR procedure. The results showed that by day 3, the levels of creatinine and the blood urea nitrogen (BUN) were significantly higher in group 3 and more significantly higher in group 2 than in group 1 (all $P < 0.0001$). The protein expression of upstream (TLR-2/TLR-4/MyD88/TRAF6/p-NF-κB) and downstream (IL-1ß/IL-6/TNF-α) inflammatory signaling molecules exhibited a pattern identical to that of creatinine levels among the groups (all $P < 0.0001$). The protein expression of oxidative stress (NOX-1/NOX-2), MAP kinase family members (ASK1/MKK4/MKK7/JNK/p-38/p-ERK1/2), apoptosis (cleaved-caspase3/cleaved-caspase8/cleaved-PARP/mitochondrial-Bax), fibrosis (Smad3/TGF-ß), and mitochondrial-damaged markers (cyclophilin D/cytosolic-cytochrome-C) displayed a pattern identical to that of creatinine levels among the groups (all $P < 0.0001$). The kidney injury score, fibrosis, cellular expression of inflammation (CD68+cells), and glomerulus/renal-tubular damaged markers (Snail/KIM-1/WT-1) exhibited an identical pattern, whereas the cellular expression of podocyte component (synaptopodin) displayed an opposite pattern of creatinine levels among the groups (all $P < 0.0001$). Therefore, the G9a inhibitor effectively protected kidneys against IR injury.

Keywords: Acute kidney ischemia-reperfusion injury, inflammation, oxidative stress, fibrosis, apoptosis, mitochondrial damage, MAPK family

Introduction

Acute kidney injury (AKI) is a universal human disease commonly encountered in patients admitted to the hospital for any reason, and its incidence is constantly rising at an alarming rate [1-4]. Despite significant improvements in critical care, medications, continuous education, renewal of the guidelines, and renal replacement therapy (RRT), the outcome of critically ill patients, especially those who are cared for in the ICU with AKI necessitating RRT

remains unacceptably poor [1-7]. It is well known that the causal etiologies of AKI are divergent, including contrast media-induced nephropathy [8, 9], shock followed by resuscitation in the emergency and intensive care settings [10, 11], kidney transplantation [12, 13], sepsis [14], cardiovascular surgery, decompensated heart failure [11, 15, 16], and toxic compound/drug exposure [11, 15].

Undoubtedly, of the aforementioned etiologies [11-16], AKI caused by ischemic and/or ischemia-reperfusion (IR) injury remains one of the most important issues to be solved in daily clinical practice [11, 13, 17]. Unfortunately, the lack of effective management remains the reason for the high incidence of patient morbidity and mortality [11, 13, 15, 17].

Abundant data have shown that the complicated mechanisms underlying AKI, especially in the setting of acute kidney IR injury, involve the generation of reactive oxygen species (ROS)/oxidative stress, mitochondrial damage [18], apoptosis [11, 13, 15, 17-19], and a cascade of inflammatory processes [17, 18, 20]. Surprisingly, although acute kidney IR injury has been identified as a common cause of AKI/acute renal failure and the underlying mechanisms have also been extensively investigated in clinical practice, it is still one of the major healthcare problems that is associated with high rates of in-hospital mortality and morbidity, regardless of advancements in current medical treatment [21-23]. This situation warrants the development of an effective and safe treatment for AKI/acute IR injury [17, 18, 20].

It is well known that histone modifications can cause the remodeling of chromatin that then mediates the activation/inactivation of gene expression. Histone methylation (HMT) is predominantly governed by the suv39h1 and G9a, which are permanent epigenetic markers [24-26]. Previous studies have revealed that G9a is correlated with malignancies in several different tumors [27-31]. In addition, in an animal model, ischemia-reperfusion has been shown to induce the upregulation of G9a and concomitant H3K9me3 modification at the Sirt1 promoter, which causes Sirt1 transcriptional suppression [32]. Of interesting is that SIRT1 is well recognized to participate in the regulation of apoptosis, the inflammatory response, oxidative stress, energy metabolism, and other processes by regulating different pathways, playing a crucial role in anti-toxicological damage as well as promoting the repair of DNA damage during replication [33-35]. BIX01294 is one of the G9a histone methyltransferase (G9a HMTase) inhibitor, which displays over 20-fold inhibition of G9a and specifically inhibits the enzyme activity of histone methyltransferase EHMT [36]. BIX01294 could also suppress cell proliferation and induce apoptosis in several different cancer types [29, 30, 36]. In contrast, suppression of G9a by BIX01294 attenuates methylglyoxal-induced tissue fibrosis, reduces renal fibrosis [37, 38] and promotes cardiac repair through generating large numbers of cardiac progenitor cells [39]. Our recent study also showed that inhibition of G9a markedly attenuated inflammation, oxidative stress, and fibrosis and preserved heart function in the setting of acute myocardial infarction in rats [40]. The aforementioned studies suggested that G9a plays different roles in different diseases and raised the hypothesis that inhibition of histone methyltransferase G9a might protect the kidney against IR injury [24-31, 37, 38, 40].

Therefore, this study focused on investigating whether the inhibition of G9a by BIX01294 could effectively preserve renal function following acute kidney ischemia-reperfusion (AKIR) injury.

Materials and methods

Ethics statement

All animal experimental procedures were approved by the Institutional Animal Care and Use Committee at Kaohsiung Chang Gung Memorial Hospital (No. 2019091602) and were performed in accordance with the Guide for the Care and Use of Laboratory Animals, 8th edition (NIH publication No. 85-23, National Academy Press, Washington, DC, USA, revised 2011). The animals were housed in an Association for Assessment and Accreditation of Laboratory Animal Care International-approved animal facility at our hospital.

Animal model of acute kidney IR injury and animal grouping

Adult male Sprague-Dawley (SD) rats weighing 320-350 g (Charles River Technology,

BioLASCO, Taipei, Taiwan) were used in this study. The procedures of acute kidney IR were performed according to our previous published studies [17, 18]. Briefly, rats (n = 24) were categorized into three groups. In Group 1, the rats underwent laparotomy only (sham-operated control (SC); laparotomy only). In the other two groups (Group 2 (acute kidney IR injury, followed by intraperitoneal administration of 1.0 cc normal saline 3 h after the procedure) and Group 3 (acute kidney IR injury + BIX01294/5 mg/kg by intraperitoneal administration at 3 h after the procedure)), the renal pedicles of the rats were clamped with non-traumatic vascular clips for 80 min, followed by reperfusion for 72 h to induce acute IR injury in both kidneys. The rats were sacrificed and their kidneys were harvested for further experiments on day 3 after the acute kidney IR procedure. The purpose of BIX01294 administration at the time point of 3 h after acute kidney IR injury was based on our daily clinical practice of AMI treatment, i.e., early reperfusion therapy and the fundamental concept of early treatment of any acute disease entity (i.e., early intervention) would offer the great benefit for the patients.

Blood sampling

Blood samples were collected from rat tail veins at baseline and 72 h after the IR procedure to measure circulating levels of creatinine and blood urea nitrogen (BUN).

Collection of 24-h urine to determine the ratio of urine protein to urine creatinine at baseline and 72 h after acute kidney IR induction

The detailed procedures are described in our previous reports [18, 41]. Briefly, each rat was placed in a metabolic cage [DXL-D, space: 190 × 290 × 550 mm^3, Suzhou Fengshi Laboratory Animal Equipment, China] for 24 h. To determine the ratio of urine protein to creatinine, 24-h urine samples were collected from all animals before and 72 h after acute kidney IR induction.

A histopathological score of kidney injury at 72 h after acute kidney IR induction

The histopathological score for kidney injury was determined in a blinded fashion, as described in our previous studies [18, 41]. Briefly, left kidney specimens from all rats were fixed in 10% buffered formalin, embedded in paraffin, sectioned at 4 μm, and stained with hematoxylin and eosin (H&E) for light microscopy. The kidney injury score [0 (none), 1 (≤ 10%), 2 (11-25%), 3 (26-45%), 4 (46-75%), and 5 (≥ 76%)] reflects the degree of tubular necrosis, loss of brush border, cast formation, and tubular dilatation.

Histological study of fibrosis

The procedures of fibrosis in kidneys were based on our previous studies [18, 41]. Briefly, we first prepared 4 μm thick serial sections of the kidney and then used Masson's trichrome staining to study fibrosis in the kidney parenchyma. Thereafter, we used Image Tool 3 (IT3) image analysis software (Image Tool for Windows, Version 3.0, University of Texas, Health Science Center, San Antonio, TX, USA) to calculate and analyze the integrated area of fibrosis in each section. Renal fibrosis was quantified as described previously [18, 41].

Immunohistochemical and immunofluorescent studies

The procedures for immunohistochemical (IHC) and immunofluorescent (IF) experiments were similar to those used in our previous studies [18, 41]. Briefly, paraffin-embedded sections were deparaffinized, rehydrated, retrieved, treated with hydrogen peroxide, incubated with primary and secondary antibodies, and finally incubated with the Envision system. According to the analytical and quantification methods used in our previous studies [18, 41], the percentage and score of positively stained cells in the kidneys were defined as follows: 0 = negative staining, 1 = < 15%, 2 = 15-25%, 3 = 25-50%, 4 = 50-75%, and 5 = 76-100%.

Antibodies and reagents

The primary and secondary antibodies used in this study were as follows: The antibodies against podocin, matrix metalloproteinase (MMP)-9, Snail, WT-1, p-Cadherin, and FSP-1 of synaptopodin were purchased from Santa Cruz Biotechnology Inc. (Dallas, TX, USA). Wilm's tumour suppressor gene 1 (WT-1), Snail, nuclear factor (NF)-κB, IL-6, oll-like receptor (TLR)-2, TLR-4, mitochondrial Bax, transforming growth factor (TGF)-ß, apoptosis signal-regulating kinase 1 (ASK1), TNF receptor associated fac-

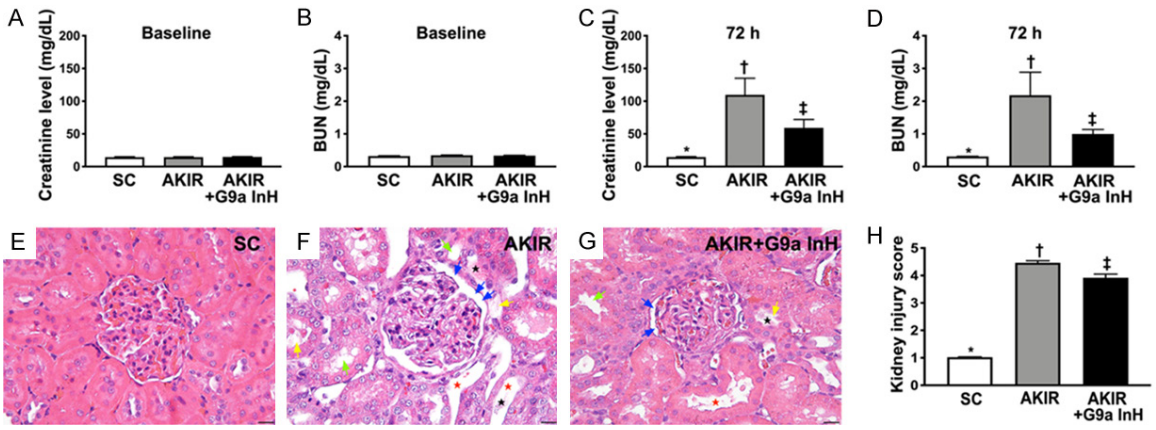

Figure 1. Blood levels of BUN and creatinine and the ratio of urine protein to urine creatinine at baseline and 72 h after acute kidney IR procedure and kidney injury. A. Baseline levels of creatinine, P > 0.5. B. Baseline levels of blood urea nitrogen (BUN), P > 0.5. C. 72 h blood levels of creatinine, *P < 0.001 vs. other groups shown with different symbols (†, ‡). D. 72 h blood levels of BUN, *P < 0.001 vs. other groups shown with different symbols (†, ‡). E-G. H&E staining for identification of kidney injury score. Light microscopic findings (400×) showing significantly higher loss of brush border in renal tubules (yellow arrows), tubular necrosis (green arrows), tubular dilatation (red asterisk) protein cast formation (black asterisk), and dilatation of Bowman's capsule (blue arrows) in IR group than that in other groups. H. Statistical results of kidney injury score, *P < 0.0001 vs. other groups shown with different symbols (†, ‡). Scale bars in the right lower corner represent 20 μm. All statistical analyses were performed by one-way ANOVA, followed by Bonferroni multiple comparison post hoc test (n = 6 for each group). Symbols (*, †, ‡) indicate significance at 0.05 level. SC: sham-operated control; IR: ischemia reperfusion; G9a InH: inhibition of histone methyltransferase G9a, i.e., BIX01294.

tor 6 (TRAF6), IKB-α, IKB-ß, Jun N-terminal kinases (JNK), myeloid differentiation primary response 88 (MyD88), CD68, cyclophilin D, nuclear factor E2-related factor 2 (Nrf2), and SIRT1 were purchased from Abcam (Boston, MA, USA). Tumor necrosis factor (TNF)-α, interleukin (IL)-1 ß, cleaved caspase 3, cleaved poly (ADP-ribose) polymerase (c-PARP), phosphorylated (p)-Smad3, mitogen-activated protein kinase 4 (MKK4), LC3B-I, LC3B-II, and the anti-rabbit immunoglobulin IgG were purchased from Cell Signaling (Beverly, MA, USA). ERK1/2, cytosolic cytochrome C, and mitochondrial cytochrome C were purchased from BD Biosciences (Billerica, MA, USA). NOX-1, NOX-2, and phosphorylated (p)-p38 were purchased from Sigma (St. Louis, MO, USA). MMK7 was purchased from Invitrogen. Kidney injury molecule (KIM)-1 was purchased from Novus (Centennial, CO, USA). Actin was purchased from Merck Ltd. (Taipei, Taiwan).

Western blot analysis

Immunoblotting was performed as previously described [18, 41]. Briefly, the protein extracts were loaded onto a sodium dodecyl sulfate-polyacrylamide gel and transferred to nitrocellulose membranes. The membranes were then incubated with primary and secondary antibodies at room temperature. Finally, the signals were developed using an Amersham ECL Western Blotting Detection Kit (Cytiva, Chicago, IL, USA) and exposed to a Biomax L film (New York, USA). ECL signals were digitized using the Labwork software (Labworks LLC, Lehi, UT, USA) for quantification.

Statistical analysis

Quantitative data are expressed as mean ± SD. Statistical analysis was performed using ANOVA followed by the Bonferroni multiple-comparison post-hoc test. SAS statistical software (SAS Institute, Cary, NC, USA) was used for statistical analysis. Statistical significance was set at P < 0.05.

Results

*Time course of circulating levels of creatinine and BUN after acute kidney IR injury and kidney injury score (**Figure 1**)*

The baseline levels of creatinine and BUN did not differ between groups 1 (SC), 2 (IR), and 3 (IR + BIX01294, a G9a inhibitor). However, 72 h after the acute kidney IR procedure, the circu-

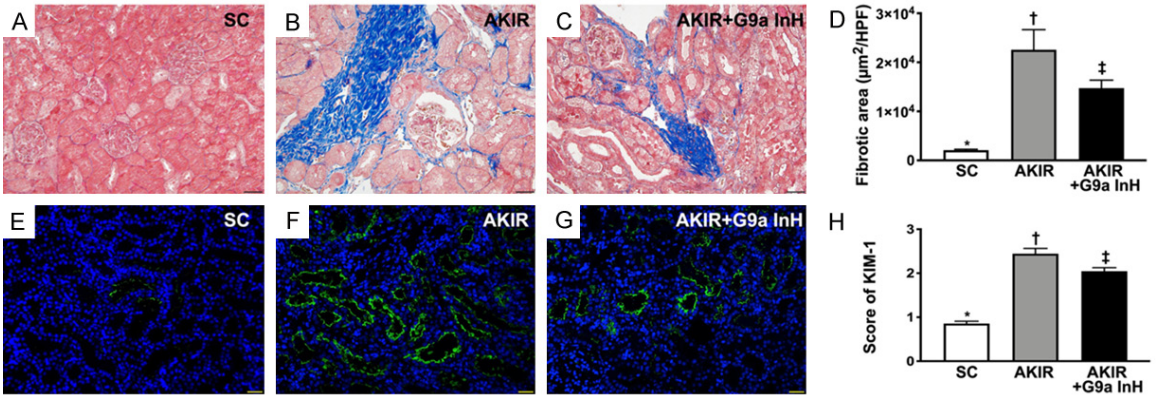

Figure 2. Histopathological finding of fibrosis and cellular kidney injury characteristics at 72 h after acute kidney IR injury. A-C. Illustration of the microscopic findings (200×) following Masson's trichrome staining for the identification of fibrotic area (blue color). Scale bars in the right lower corner represent 50 μm. D. Statistical results of fibrotic area, *P < 0.0001 vs. other groups shown with different symbols (†, ‡). E-G. Illustration of the immunofluorescent microscopic findings (400×) for identification of expression of kidney injury molecule (KIM)-1 (green color). Scale bars in right lower corner represent 20 μm. H. Statistical results of KIM-1 score expression, *P < 0.0001 vs. other groups shown with different symbols (†, ‡). All statistical analyses were performed by one-way ANOVA, followed by Bonferroni multiple comparison post hoc test (n = 6 for each group). Symbols (*, †, ‡) indicate significance at 0.05 level. SC: sham-operated control; IR: ischemia reperfusion; G9a InH: inhibition of histone methyltransferase G9a, i.e., BIX01294.

lating levels of BUN and creatinine were significantly higher in Group 2 than those in Groups 1 and 3, and significantly higher in Group 3 than those in Group 1.

To elucidate whether the G9a inhibitor effectively protected the integrity of the kidney parenchyma, microscopic analysis of H&E staining was performed. The results demonstrated that the kidney injury score was significantly higher in Group 2 than that in Group 1, which was significantly reversed in Group 3, suggesting that BIX01294 effectively protected the integrity of the kidney parenchyma.

*The histopathological finding of fibrosis and cellular effects of kidney injury at 72 h after acute kidney IR injury (**Figure 2**)*

To determine whether fibrosis develops within 72 h after acute kidney injury, Masson's trichrome staining was performed. The results showed that the fibrotic area was significantly increased in Group 2 compared to that in Groups 1 and 3, and significantly increased in Group 3 compared to that in Group 1.

Thereafter, we examined the cellular expression of KIM-1, a typical biomarker of renal tubular injury, using immunofluorescence microscopy. The results showed that this parameter exhibited an identical pattern of fibrosis in the three groups.

*Identification of renal tubular and glomerular damage markers at 72 h after acute kidney IR injury (**Figure 3**)*

We used the IHC staining to further examine whether the cellular levels of renal tubular and glomerular injury markers were upregulated in this study. The results showed that the expression of snail, predominantly in the tubular nuclei, and the expression of WT-1, predominantly in podocytes, were significantly increased in Group 2 compared to Group 1, which was significantly reversed in Group 3, suggesting that treatment with BIX01294 remarkably attenuated kidney tissue damage not only in the renal tubules but also in the glomerular ultrastructure.

*Identification of podocyte component and inflammatory cell infiltration at 72 h after acute kidney IR injury (**Figure 4**)*

We also used the IF staining to clarify whether synaptopodin, a component of the podocyte foot process, was preserved in the IR kidney undergoing G9a inhibitor treatment in this study. The results showed that synaptopodin was significantly lower in Group 2 than that in Groups 1 and 3, and significantly lower in Group 3 than that in Group 1. Additionally, the cellular expression of CD68, an indicator of inflammation, exhibited a pattern identical to

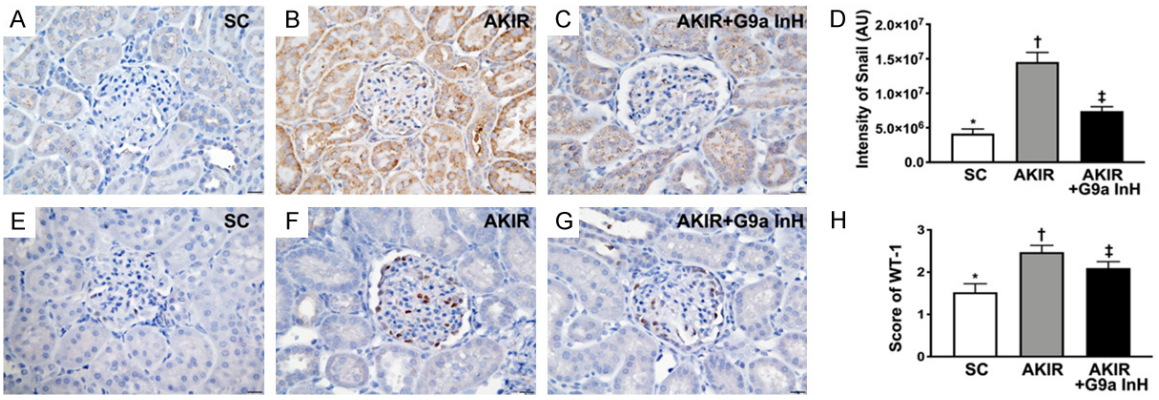

Figure 3. Microscopic findings for the identification of renal tubular and glomerular damage biomarkers at 72 h after acute kidney IR injury. A-C. Illustration of the immunohistochemical (IHC) microscopic findings (400×) regarding the expression of Snail (gray color). D. Statistical results of the fluorescent intensity of Snail, *P < 0.0001 vs. other groups shown with different symbols (†, ‡). E-G. Illustration of the IHC microscopic findings (400×) regarding the expression of Wilm's tumor suppressor gene 1 (WT-1) (gray color). H. Statistical result of WT-1 expression score, *P < 0.0001 vs. other groups shown with different symbols (†, ‡). Scale bars in the right lower corner represent 20 μm. All statistical analyses were performed by one-way ANOVA, followed by Bonferroni multiple comparison post hoc test (n = 6 for each group). Symbols (*, †, ‡) indicate significance at 0.05 level. SC: sham-operated control; IR: ischemia reperfusion; G9a InH: inhibition of histone methyltransferase G9a, i.e., BIX01294.

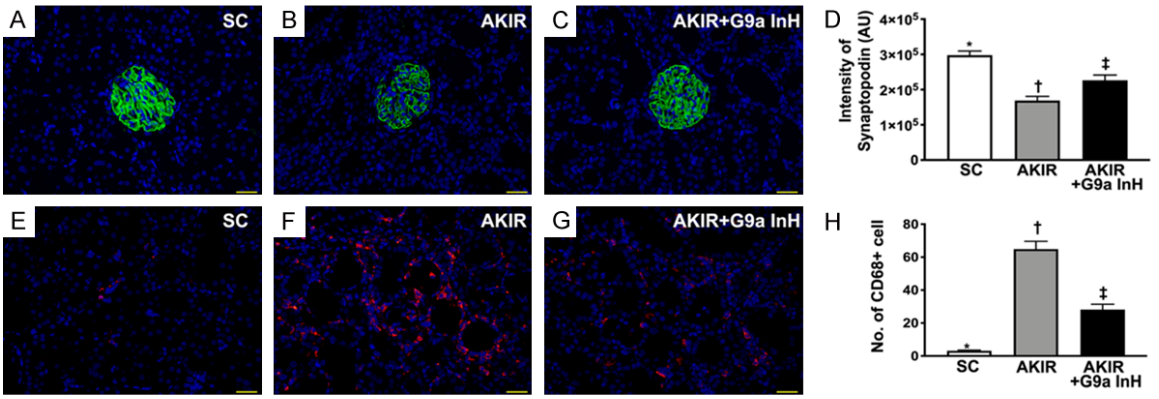

Figure 4. Microscopic findings for the identification of podocyte component and inflammatory cell infiltration at 72 h after acute kidney IR procedure. A-C. Illustration of immunofluorescent (IF) microscopic findings (400×) for the identification of synaptopodin in renal glomerulus (green color). D. Statistical results of the fluorescent intensity of synaptopodin staining, *P < 0.0001 vs. other groups shown with different symbols (†, ‡). E-G. Illustration of the IF microscopic findings for the identification of cellular expression of CD68 (red color). H. Statistical results of the number of CD68 positively stained cells, *P < 0.0001 vs. other groups shown with different symbols (†, ‡). Scale bars in right lower corner represent 20 μm. All statistical analyses were performed by one-way ANOVA, followed by Bonferroni multiple comparison post hoc test (n = 6 for each group). Symbols (*, †, ‡) indicate significance at 0.05 level. SC: sham-operated control; IR: ischemia reperfusion; G9a InH: inhibition of histone methyltransferase G9a, i.e., BIX01294.

that of synaptopodin expression among the groups.

*BIX01294 treatment suppressed the expression of inflammatory signaling proteins upstream and downstream at 72 h after acute kidney IR injury (**Figure 5**)*

To delineate whether G9a inhibitor treatment downregulates the upstream and downstream inflammatory signaling molecules, western blot analysis was performed. As expected, the protein expression levels of TLR-2, TLR-4, MyD88, TRAF6, and p-NF-κB, five indices of upstream inflammatory signaling, and the protein expression levels of IL-1ß, IL-6, and TNF-α, three indices of downstream inflammatory signaling, were significantly higher in Group 2 than those in Groups 1 and 3, and significantly higher in

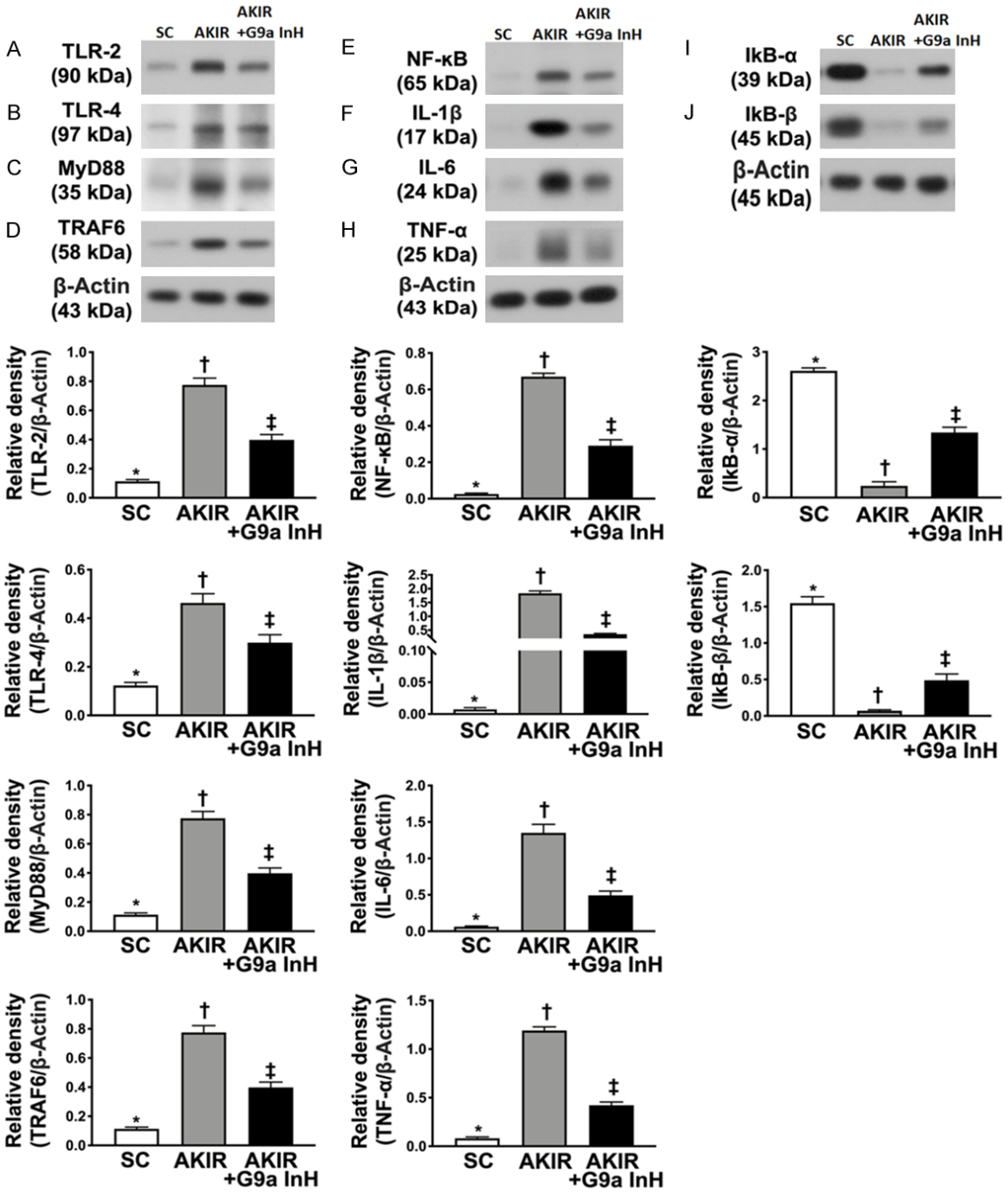

Figure 5. BIX01294 treatment suppressed the protein expressions of upstream and downstream signaling molecules at 72 h after acute kidney IR injury. A. Protein expression of toll-like receptor (TLR)-2, *P < 0.0001 vs. other groups shown with different symbols (†, ‡). B. Protein expression of TLR-4, *P < 0.0001 vs. other groups shown with different symbols (†, ‡). C. Protein expression of myeloid differentiation primary response 88 (MyD88), *P < 0.0001 vs. other groups shown with different symbols (†, ‡). D. Protein expression of tumor necrosis factor (TNF) receptor-associated factor 6 (TRAF6), *P < 0.0001 vs. other groups shown with different symbols (†, ‡). E. Protein expression of phosphorylated nuclear factor (p-NF)-κB, *P < 0.0001 vs. other groups shown with different symbols (†, ‡). F. Protein expression of interleukin (IL)-1ß, *P < 0.0001 vs. other groups shown with different symbols (†, ‡). G. Protein expression of IL-6, *P < 0.0001 vs. other groups shown with different symbols (†, ‡). H. Protein expression of tumor necrosis factor (TNF)-α, *P < 0.0001 vs. other groups shown with different symbols (†, ‡). I. Protein expression of IKB-α, *P < 0.0001 vs. other groups shown with different symbols (†, ‡). J. Protein expression of IKB-ß, *P < 0.0001 vs. other groups shown with different symbols (†, ‡). All statistical analyses were performed by one-way ANOVA, followed by Bonferroni multiple comparison post hoc test (n = 6 for each group). Symbols (*, †, ‡) indicate significance at 0.05 level. SC: sham-operated control; IR: ischemia reperfusion; G9a InH: inhibition of histone methyltransferase G9a, i.e., BIX01294.

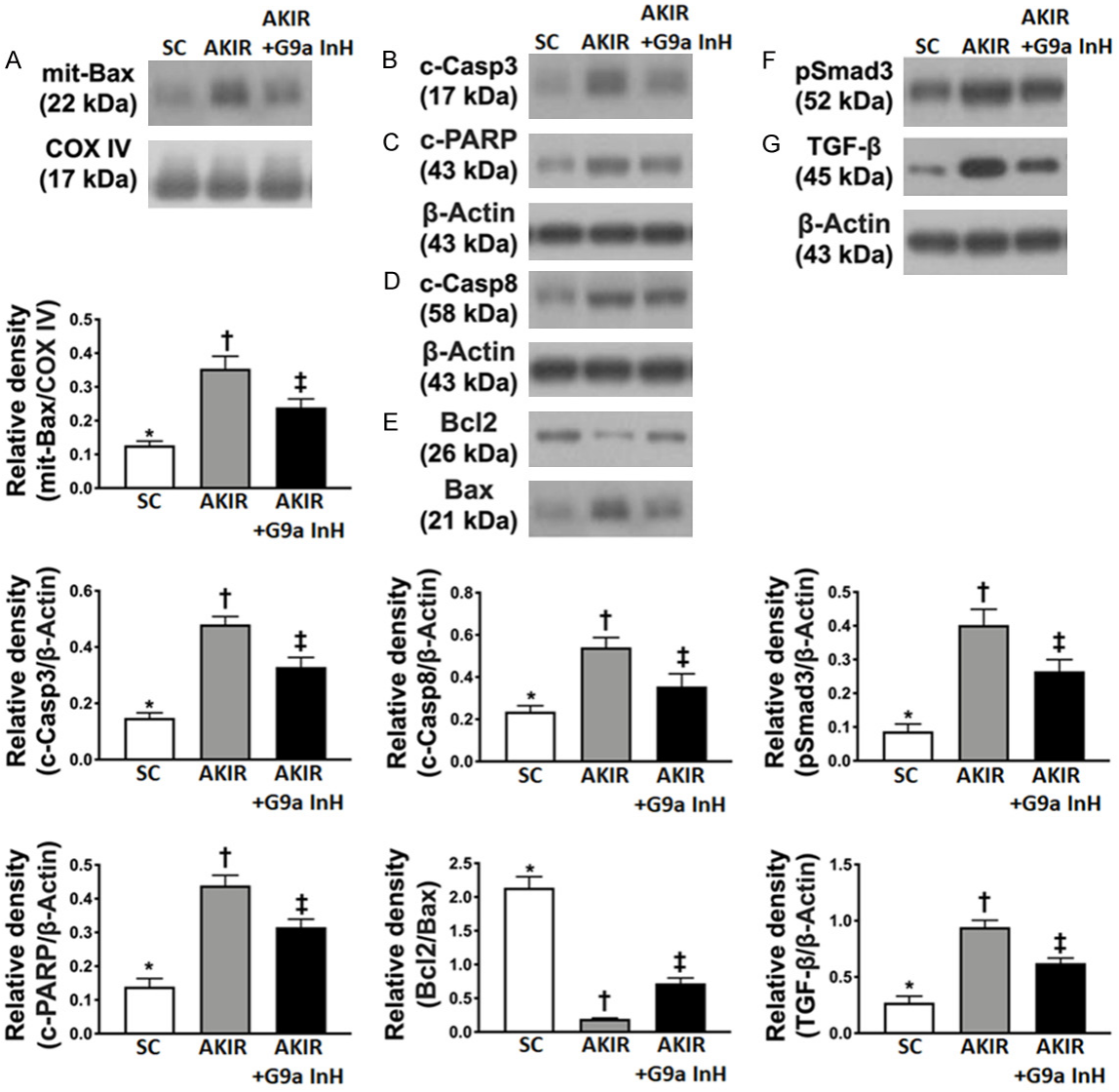

Figure 6. BIX01294 treatment attenuated the expression of apoptosis and fibrosis proteins at 72 h after acute kidney IR injury. A. Protein expression of mitochondrial (mito)-Bax, *P < 0.0001 vs. other groups shown with different symbols (†, ‡). B. Protein expression of cleaved caspase 3 (c-Casp3), *P < 0.0001 vs. other groups shown with different symbols (†, ‡). C. Protein expression of caspase 8 (Casp8), *P < 0.0001 vs. other groups shown with different symbols (†, ‡). D. Protein expression of cleaved poly (ADP-ribose) polymerase (c-PARP), *P < 0.0001 vs. other groups shown with different symbols (†, ‡). E. The ratio of Bcl-2 protein levels to those of Bax, *P < 0.0001 vs. other groups shown with different symbols (†, ‡). F. Protein expression of Smad3, *P < 0.0001 vs. other groups shown with different symbols (†, ‡). G. Protein expression of transforming growth factor (TGF)-ß, *P < 0.0001 vs. other groups shown with different symbols (†, ‡). All statistical analyses were performed by one-way ANOVA, followed by Bonferroni multiple comparison post hoc test (n = 6 for each group). Symbols (*, †, ‡) indicate significance at 0.05 level. SC: sham-operated control; IR: ischemia reperfusion; G9a InH: inhibition of histone methyltransferase G9a, i.e., BIX01294.

Group 3 than those in Group 1. However, the protein expression levels of IKB-α and IKB-ß, two inhibitors of the transmission of the upstream inflammatory signaling into the downstream inflammatory signaling, exhibited an opposite pattern among the three groups.

*BIX01294 treatment reduced expression of apoptosis and fibrosis related at 72 h after acute kidney IR injury (**Figure 6**)*

To examine whether the Ga9 inhibitor would attenuate apoptotic, fibrotic, and autophagic

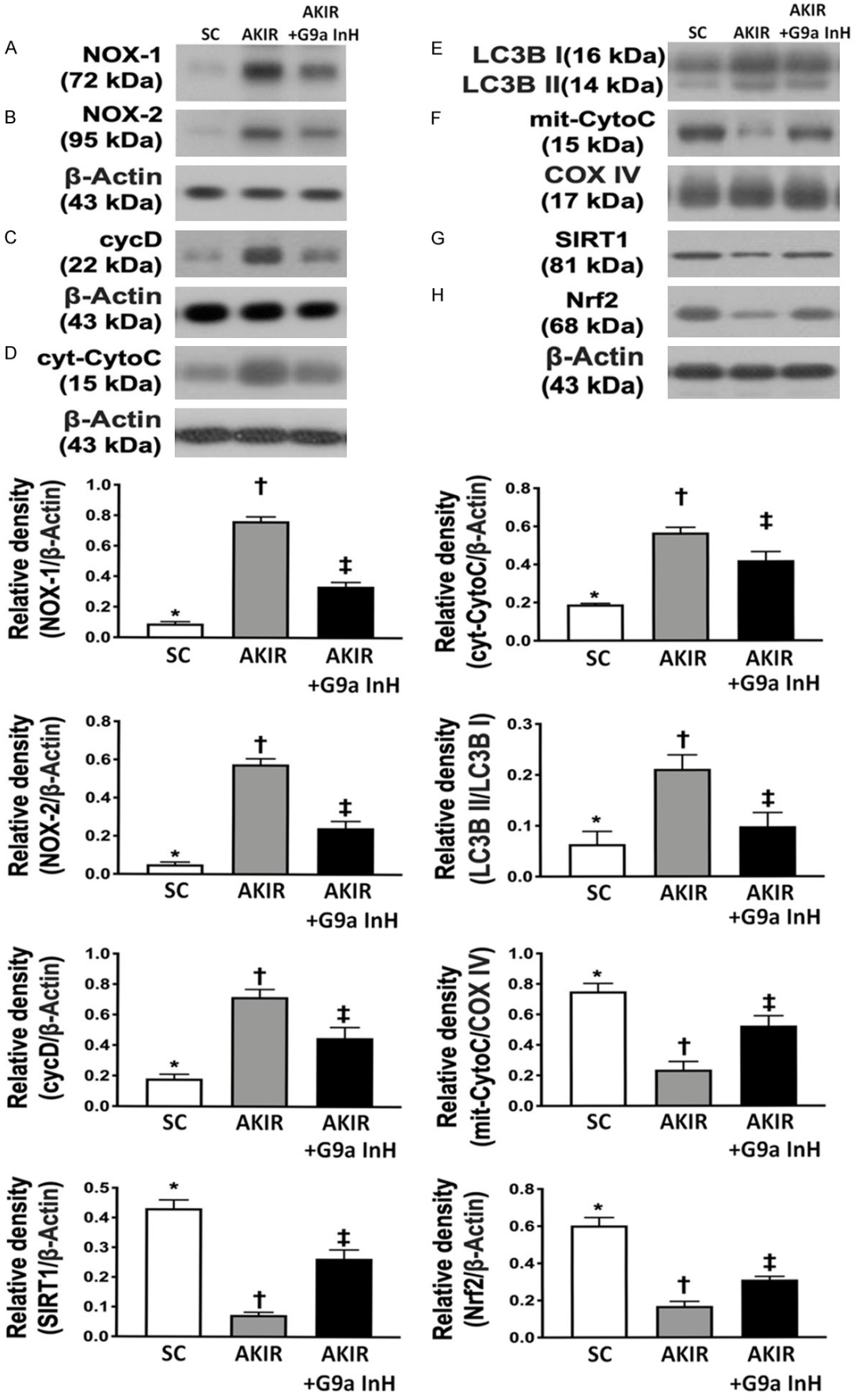
SC
AKIR
AKIR +G9a InH
A
NOX-1 (72 kDa)
B
NOX-2 (95 kDa)
β-Actin (43 kDa)
C
cycD (22 kDa)
β-Actin (43 kDa)
D
cyt-CytoC (15 kDa)
β-Actin (43 kDa)
E
LC3B I(16 kDa)
LC3B II(14 kDa)
F
mit-CytoC (15 kDa)
COX IV (17 kDa)
G
SIRT1 (81 kDa)
H
Nrf2 (68 kDa)
β-Actin (43 kDa)
Relative density (NOX-1/β-Actin)
Relative density (cyt-CytoC/β-Actin)
Relative density (NOX-2/β-Actin)
Relative density (LC3B II/LC3B I)
Relative density (cycD/β-Actin)
Relative density (mit-CytoC/COX IV)
Relative density (SIRT1/β-Actin)
Relative density (Nrf2/β-Actin)
SC
AKIR
AKIR +G9a InH

Figure 7. BIX01294 treatment restrained the oxidative stress, mitochondrial damage and autophagy at 72 h after acute kidney IR injury. A. Protein expression of NOX-1, *P < 0.0001 vs. other groups shown with different symbols (†, ‡). B. Protein expression of NOX-2, *P < 0.0001 vs. other groups shown with different symbols (†, ‡). C. Protein expressions of cyclophilin D (cycD), *P < 0.0001 vs. other groups shown with different symbols (†, ‡). D. Protein expression of cytosolic cytochrome C (cyt-CytoC), *P < 0.0001 vs. other groups shown with different symbols (†, ‡). E. The ratio of the levels of LC3B-II to those of LC3B-I, *P < 0.0001 vs. other groups with different symbols (†, ‡). F. Protein expression of mitochondrial cytochrome C (mit-CytoC), *P < 0.0001 vs. other groups shown with different symbols (†, ‡). G. Protein expression of SIRT1, *P < 0.0001 vs. other groups with different symbols (†, ‡). H. Nuclear factor E2-related factor 2 (Nrf2), *P < 0.0001 vs. other groups with different symbols (†, ‡). All statistical analyses were performed by one-way ANOVA, followed by Bonferroni multiple comparison post hoc test (n = 6 for each group). Symbols (*, †, ‡) indicate significance at 0.05 level. SC = sham-operated control; IR = ischemia reperfusion; G9a InH = inhibition of histone methyltransferase G9a, i.e., BIX01294.

biomarkers, western blot analysis was performed. As expected, the expressions of mitochondrial Bax, cleaved caspase 3, caspase 8, and cleaved PARP proteins, four indicators of apoptosis, were significantly higher in Group 2 than those in Groups 1 and 3, and significantly higher in Group 3 than those in Group 1. In contrast, the ratio of the levels of Bcl-2 to those of Bax, an inhibitor of cytochrome C release from the mitochondria to the cytosol, exhibited an opposite pattern of caspase 3 among the three groups.

Additionally, the expression of Smad3 and TGF-β proteins, two indicators of fibrosis, displayed an identical pattern of apoptosis among the three groups.

*BIX01294 treatment restrained oxidative stress, mitochondrial damage, and autophagy at 72 h after the acute kidney IR procedure (**Figure 7**)*

The expression of NOX-1 and NOX-2 proteins, two indicators of oxidative stress, was significantly higher in Group 2 than that in Groups 1 and 3 and significantly higher in Group 3 than that in Group 1. Additionally, the expression of cyclophilin D and cytosolic cytochrome C proteins, two indicators of mitochondrial damage, exhibited identical patterns of oxidative stress among the three groups. Additionally, the ratio of the expression levels of LC3B-II to those of LC3B-I, an indicator of autophagy, also exhibited an identical pattern of oxidative stress among the groups. In contrast, the expression of mitochondrial cytochrome C protein, an indicator of mitochondrial integrity, displayed an opposite pattern of oxidative stress. Furthermore, the protein expression of Nrf2 and SIRT1, two cardinal proteins that protect the cells/tissues against oxidative stress [33], was significantly lower in group 2 than that in groups 1 and 3 and significantly lower in group 3 than that in group 1, suggesting that BIX01294 treatment could enhance the expression of antioxidant in kidney parenchyma through upregulation of SIRT1.

*BIX01294 treatment regulated the MAPK family signaling at 72 h after acute kidney IR injury (**Figure 8**)*

To examine whether MAPK family members were also upregulated in acute kidney IR injury and whether G9a inhibitor treatment downregulated the expression of MAPK family members, western blot analysis was performed. The results demonstrated that the expression of ASK1, MMK4, MMK7, JNK, p-p38, and ERK1/2 proteins, six members of the MAP kinase family that are involved in directing cellular responses to a diverse array of stimuli, was significantly increased in Group 2 compared to that in Group 1, which was significantly reversed in Group 3, suggesting that G9a inhibitor treatment effectively downregulated this signaling pathway.

Discussion

This study, which investigated the therapeutic impact of a G9a inhibitor on protecting kidney architecture and functional integrity against acute kidney IR, yielded several striking results. First, at least two signaling pathways, the upstream and downstream inflammatory signaling pathway and the oxidative stress-mitogen activated protein kinase pathway, were identified to directly participate in kidney damage in acute kidney IR. Second, inhibition of G9a inhibitor effectively protected kidney architecture and functional integrity, raising the possibility for the future application of this approach in AKI/IR injury patients, especially those who are refractory to traditional management.

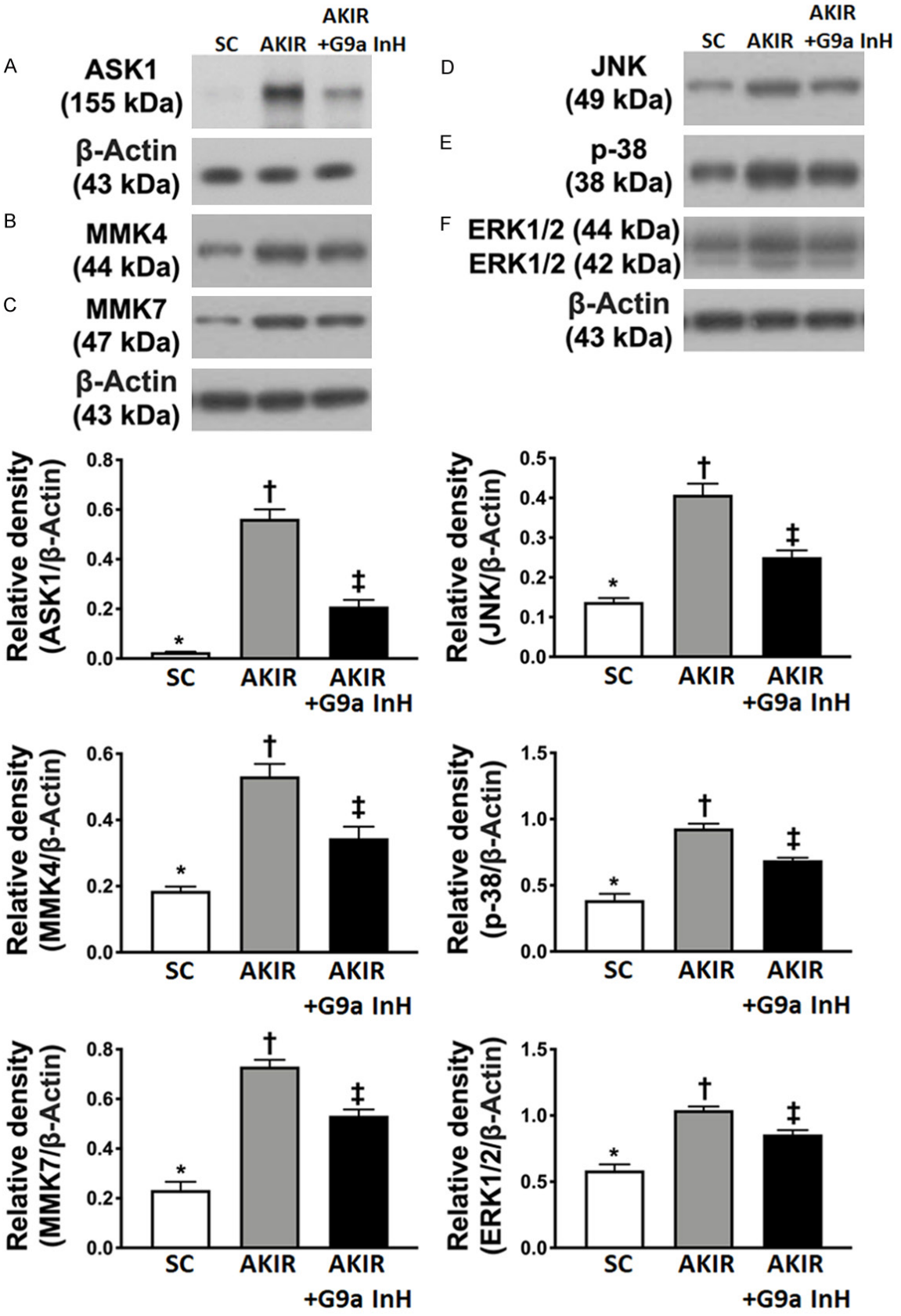

Figure 8. BIX01294 treatment regulated the MAPK family signaling at 72 h after acute kidney IR procedure. A. Protein expression of Apoptosis signal-regulating kinase 1 (ASK1), *P < 0.0001 vs. other groups shown with different

symbols (†, ‡). B. Protein expression of MMK4, *P < 0.0001 vs. other groups shown with different symbols (†, ‡). C. Protein expression of MMK7, *P < 0.0001 vs. other groups shown with different symbols (†, ‡). D. Protein expression of Jun N-terminal kinase (JNK), *P < 0.0001 vs. other groups shown with different symbols (†, ‡). E. Protein expression of phosphorylated (p)-p38, *P < 0.0001 vs. other groups shown with different symbols (†, ‡). F. Protein expression of ERK1/2, *P < 0.0001 vs. other groups shown with different symbols (†, ‡). All statistical analyses were performed by one-way ANOVA, followed by Bonferroni multiple comparison post hoc test (n = 6 for each group). Symbols (*, †, ‡) indicate significance at 0.05 level. SC: sham-operated control; IR: ischemia reperfusion; G9a InH: inhibition of histone methyltransferase G9a, i.e., BIX01294.

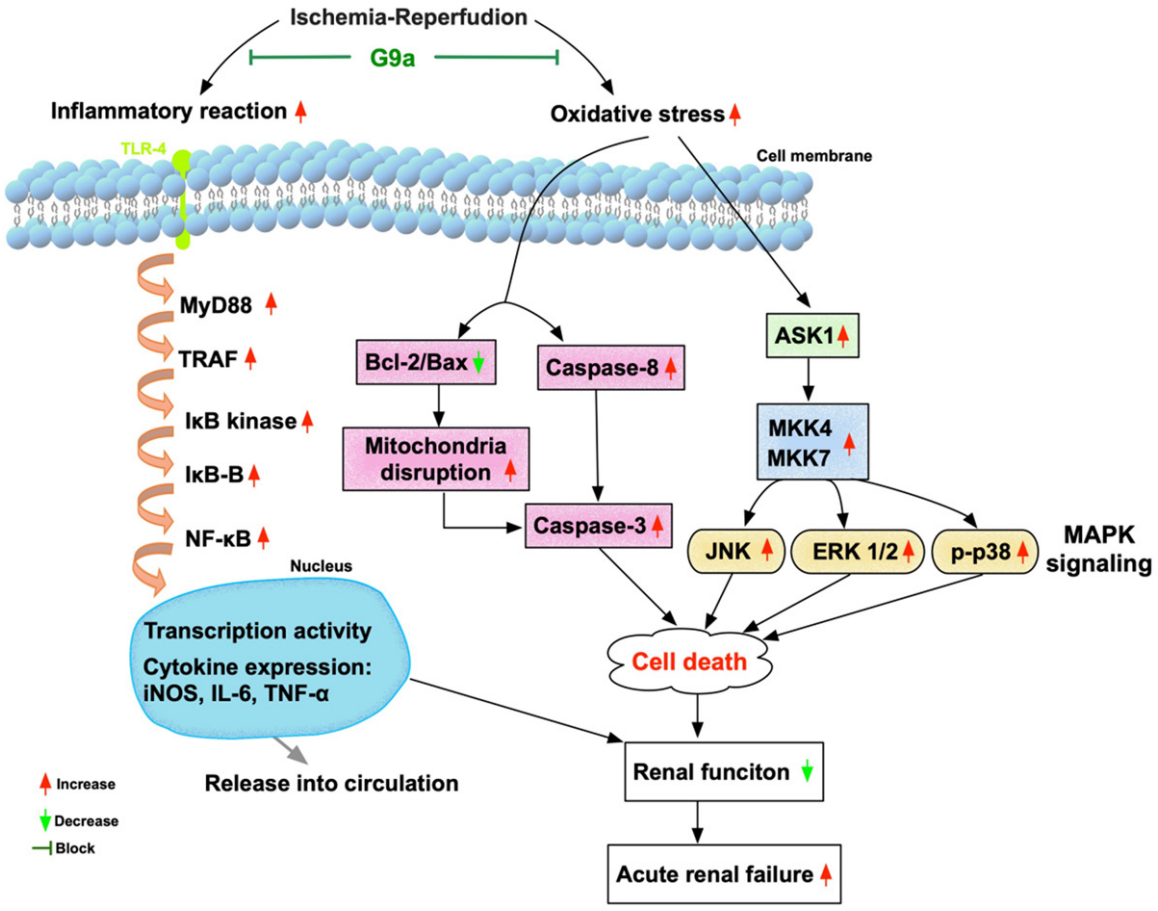

Figure 9. Schematic illustrating the underlying mechanisms of G9a inhibitor treatment in protecting the acute kidney injury against ischemia-reperfusion injury.

Interestingly, our recent study demonstrated that BIX01294, a histone methyltransferase G9a inhibitor, effectively protected the myocardium and heart function in acute myocardial infarction in rodents [41]. The most important finding of the present study was that the kidney injury score (an anatomically pathological feature) was remarkably higher in IR animals than that in SC animals, which was remarkably reversed in IR animals treated with BIX01294. Additionally, the circulating levels of BUN and creatinine along with the ratio of urine protein to urine creatinine (renal function parameters) were also substantially increased in IR animals compared to those in SC animals, which were substantially reversed in IR animals after receiving BIX01294 treatment. Accordingly, our findings support the results of a recent study [40].

Abundant data have shown that etiologies [8-17] are multifactorial, but the underlying mechanisms are complicated in the setting of AKI/IR injury [17, 18, 41]. Additionally, evidence has revealed that organ ischemia and tissue necrosis frequently elicit inflammatory reac-

tions and oxidative stress, which further contribute to organ damage and cell death [17, 18, 41-43]. An essential finding of the present study was that both upstream and downstream inflammatory signaling molecules were markedly upregulated in IR animals (**Figure 9**). Additionally, oxidative stress-MAPK family signaling was notably augmented in IR animals (**Figure 9**). Our findings, in addition to being consistent with the findings of previous studies [17, 18, 41-43], could fundamentally explain why renal function and architecture in IR animals were seriously damaged and why fibrosis, apoptosis, and mitochondria damage in the kidney were substantially enhanced in IR animals. Importantly, the molecular and cellular changes as well as organelle and tissue perturbations were significantly reversed in IR animals treated with BIX01294.

Undoubtedly, the exact underlying mechanism of how the BIX01294 (i.e., G9a inhibitor) treatment protects the kidney against IR injury could be most interesting for the readers. Although our recent study has also revealed that suppressing the G9a expression could substantially ameliorate the inflammatory reaction and generation of oxidative stress in AMI rodent [40], what was the precise mechanism of such a treatment in protecting the heart organ was not clearly identified. Interestingly, recent study has revealed that Nrf2 and SIRT1, two cardinal antioxidant proteins that protect the cells/tissues against oxidative stress [33] through regulating the NF-κB, suppress the toxic damage process of toxicants by the downregulating the inflammatory response and oxidative stress. Intriguingly, the result of the present study displayed that as compared to the IR animals the protein expressions of SIRT1 and Nrf2 were remarkably upregulated in IR animals after receiving BIX01294 treatment. Perhaps, our finding and the findings from recent study [33] could more precisely explain why the BIX01294 therapy could promisingly protect the kidney against IR injury. Thus, based on the results of our study, we schematically proposed the underlying mechanism of the BIX01294 therapy for attenuating the kidney injury in the setting of acute kidney IR in rat.

Conclusion

The results of the present study demonstrated that BIX01294 effectively protected kidney architecture and renal functional integrity against acute kidney IR injury in rodents.

Acknowledgements

This study were supported by a program grant from Kaohsiung Chang Gung Memorial Hospital, Chang Gung University [grant number: CMRPG8K0681] and a research grant from Kaohsiung Medical University Hospital (KMUH110-0R41).

Disclosure of conflict of interest

None.

Address correspondence to: Honkan Yip, Division of Cardiology, Department of Internal Medicine, Kaohsiung Chang Gung Memorial Hospital, Kaohsiung 83301, Taiwan. Tel: +886-7-7317123; Fax: +886-7-7322402; E-mail: han.gung@msa.hinet.net; Chiwen Luo, Department of Surgery, Kaohsiung Medical University Hospital, 100 Tzyou 1st Road, Kaohsiung 80756, Taiwan. Tel: +886-7-3121101 Ext. 2260; Fax: +886-7-3165011; E-mail: cwlo0623@gmail.com

References

[1] Floege J JR and Feehally J. Comprehensive clinical nephrology. 2010.
[2] Kumar A and Singh NP. Antimicrobial dosing in critically ill patients with sepsis-induced acute kidney injury. Indian J Crit Care Med 2015; 19: 99-108.
[3] Murray PT. Acute kidney injury and critical care nephrology. NephSAP 2013; 12: 77-152.
[4] Reichel RR. Acute kidney injury: quoi de neuf? Ochsner J 2014; 14: 359-368.
[5] KDIGO. Acute Kidney Injury Work Group. KDIGO clinical practice guidelines for acute kidney injury. Kidney Int Suppl 2012; 2: 1-138.
[6] Hoste EA and De Corte W. Implementing the kidney disease: improving global outcomes/acute kidney injury guidelines in ICU patients. Curr Opin Crit Care 2013; 19: 544-553.
[7] Mehta RL, Kellum JA, Shah SV, Molitoris BA, Ronco C, Warnock DG and Levin A. Acute kidney injury network: report of an initiative to improve outcomes in acute kidney injury. Crit Care 2007; 11: R31.
[8] Lameire N and Kellum JA. Contrast-induced acute kidney injury and renal support for acute kidney injury: a KDIGO summary (Part 2). Crit Care 2013; 17: 205.
[9] Parikh CR, Coca SG, Wang Y, Masoudi FA and Krumholz HM. Long-term prognosis of acute

kidney injury after acute myocardial infarction. Arch Intern Med 2008; 168: 987-995.
[10] Di Nardo M, Ficarella A, Ricci Z, Luciano R, Stoppa F, Picardo S, Picca S, Muraca M and Cogo P. Impact of severe sepsis on serum and urinary biomarkers of acute kidney injury in critically ill children: an observational study. Blood Purif 2013; 35: 172-176.
[11] Friedericksen DV, Van der Merwe L, Hattingh TL, Nel DG and Moosa MR. Acute renal failure in the medical ICU still predictive of high mortality. S Afr Med J 2009; 99: 873-875.
[12] Jang HR, Ko GJ, Wasowska BA and Rabb H. The interaction between ischemia-reperfusion and immune responses in the kidney. J Mol Med (Berl) 2009; 87: 859-864.
[13] Sementilli A and Franco M. Renal acute cellular rejection: correlation between the immunophenotype and cytokine expression of the inflammatory cells in acute glomerulitis, arterial intimitis, and tubulointerstitial nephritis. Transplant Proc 2010; 42: 1671-1676.
[14] Bagshaw SM, Bennett M, Haase M, Haase-Fielitz A, Egi M, Morimatsu H, D'Amico G, Goldsmith D, Devarajan P and Bellomo R. Plasma and urine neutrophil gelatinase-associated lipocalin in septic versus non-septic acute kidney injury in critical illness. Intensive Care Med 2010; 36: 452-461.
[15] Lameire N, Van Biesen W and Vanholder R. Acute renal failure. Lancet 2005; 365: 417-430.
[16] Morgan CJ, Gill PJ, Lam S and Joffe AR. Perioperative interventions, but not inflammatory mediators, increase risk of acute kidney injury after cardiac surgery: a prospective cohort study. Intensive Care Med 2013; 39: 934-941.
[17] Chen YT, Sun CK, Lin YC, Chang LT, Chen YL, Tsai TH, Chung SY, Chua S, Kao YH, Yen CH, Shao PL, Chang KC, Leu S and Yip HK. Adipose-derived mesenchymal stem cell protects kidneys against ischemia-reperfusion injury through suppressing oxidative stress and inflammatory reaction. J Transl Med 2011; 9: 51.
[18] Chen YT, Tsai TH, Yang CC, Sun CK, Chang LT, Chen HH, Chang CL, Sung PH, Zhen YY, Leu S, Chang HW, Chen YL and Yip HK. Exendin-4 and sitagliptin protect kidney from ischemia-reperfusion injury through suppressing oxidative stress and inflammatory reaction. J Transl Med 2013; 11: 270.
[19] da Silva LB, Palma PV, Cury PM and Bueno V. Evaluation of stem cell administration in a model of kidney ischemia-reperfusion injury. Int Immunopharmacol 2007; 7: 1609-1616.
[20] Li B, Cohen A, Hudson TE, Motlagh D, Amrani DL and Duffield JS. Mobilized human hematopoietic stem/progenitor cells promote kidney repair after ischemia/reperfusion injury. Circulation 2010; 121: 2211-2220.
[21] Ali T, Khan I, Simpson W, Prescott G, Townend J, Smith W and Macleod A. Incidence and outcomes in acute kidney injury: a comprehensive population-based study. J Am Soc Nephrol 2007; 18: 1292-1298.
[22] Thadhani R, Pascual M and Bonventre JV. Acute renal failure. N Engl J Med 1996; 334: 1448-1460.
[23] Xue JL, Daniels F, Star RA, Kimmel PL, Eggers PW, Molitoris BA, Himmelfarb J and Collins AJ. Incidence and mortality of acute renal failure in Medicare beneficiaries, 1992 to 2001. J Am Soc Nephrol 2006; 17: 1135-1142.
[24] Jenuwein T and Allis CD. Translating the histone code. Science 2001; 293: 1074-1080.
[25] Martin C and Zhang Y. The diverse functions of histone lysine methylation. Nat Rev Mol Cell Biol 2005; 6: 838-849.
[26] Shi Y and Whetstine JR. Dynamic regulation of histone lysine methylation by demethylases. Mol Cell 2007; 25: 1-14.
[27] Baxter E, Windloch K, Gannon F and Lee JS. Epigenetic regulation in cancer progression. Cell Biosci 2014; 4: 45.
[28] Huang J and Berger SL. The emerging field of dynamic lysine methylation of non-histone proteins. Curr Opin Genet Dev 2008; 18: 152-158.
[29] Luo CW, Wang JY, Hung WC, Peng G, Tsai YL, Chang TM, Chai CY, Lin CH and Pan MR. G9a governs colon cancer stem cell phenotype and chemoradioresistance through PP2A-RPA axis-mediated DNA damage response. Radiother Oncol 2017; 124: 395-402.
[30] Pan MR, Hsu MC, Luo CW, Chen LT, Shan YS and Hung WC. The histone methyltransferase G9a as a therapeutic target to override gemcitabine resistance in pancreatic cancer. Oncotarget 2016; 7: 61136-61151.
[31] Tsai YP and Wu KJ. Epigenetic regulation of hypoxia-responsive gene expression: focusing on chromatin and DNA modifications. Int J Cancer 2014; 134: 249-256.
[32] Liu H, Wang W, Weng X, Chen H, Chen Z, Du Y, Liu X and Wang L. The H3K9 histone methyltransferase G9a modulates renal ischemia reperfusion injury by targeting Sirt1. Free Radic Biol Med 2021; 172: 123-135.
[33] Ren Z, He H, Zuo Z, Xu Z, Wei Z and Deng J. The role of different SIRT1-mediated signaling pathways in toxic injury. Cell Mol Biol Lett 2019; 24: 36.
[34] Li X, Zhang S, Blander G, Tse JG, Krieger M and Guarente L. SIRT1 deacetylates and positively regulates the nuclear receptor LXR. Mol Cell 2007; 28: 91-106.
[35] Oberdoerffer P, Michan S, McVay M, Mostoslavsky R, Vann J, Park SK, Hartlerode A, Stegmuller J, Hafner A, Loerch P, Wright SM, Mills KD, Bonni A, Yankner BA, Scully R, Prolla TA, Alt

FW and Sinclair DA. SIRT1 redistribution on chromatin promotes genomic stability but alters gene expression during aging. Cell 2008; 135: 907-918.

[36] Bellamy J, Szemes M, Melegh Z, Dallosso A, Kollareddy M, Catchpoole D and Malik K. Increased efficacy of histone methyltransferase G9a inhibitors against MYCN-amplified neuroblastoma. Front Oncol 2020; 10: 818.

[37] Irifuku T, Doi S, Sasaki K, Doi T, Nakashima A, Ueno T, Yamada K, Arihiro K, Kohno N and Masaki T. Inhibition of H3K9 histone methyltransferase G9a attenuates renal fibrosis and retains klotho expression. Kidney Int 2016; 89: 147-157.

[38] Maeda K, Doi S, Nakashima A, Nagai T, Irifuku T, Ueno T and Masaki T. Inhibition of H3K9 methyltransferase G9a ameliorates methylglyoxal-induced peritoneal fibrosis. PLoS One 2017; 12: e0173706.

[39] Kaur K, Yang J, Edwards JG, Eisenberg CA and Eisenberg LM. G9a histone methyltransferase inhibitor BIX01294 promotes expansion of adult cardiac progenitor cells without changing their phenotype or differentiation potential. Cell Prolif 2016; 49: 373-385.

[40] Sung PH, Luo CW, Chiang JY and Yip HK. The combination of G9a histone methyltransferase inhibitors with erythropoietin protects heart against damage from acute myocardial infarction. Am J Transl Res 2020; 12: 3255-3271.

[41] Yip HK, Yang CC, Chen KH, Huang TH, Chen YL, Zhen YY, Sung PH, Chiang HJ, Sheu JJ, Chang CL, Chen CH, Chang HW and Chen YT. Combined melatonin and exendin-4 therapy preserves renal ultrastructural integrity after ischemia-reperfusion injury in the male rat. J Pineal Res 2015; 59: 434-447.

[42] Lin KC, Wallace CG, Yin TC, Sung PH, Chen KH, Lu HI, Chai HT, Chen CH, Chen YL, Li YC, Shao PL, Lee MS, Sheu JJ and Yip HK. Shock wave therapy enhances mitochondrial delivery into target cells and protects against acute respiratory distress syndrome. Mediators Inflamm 2018; 2018: 5425346.

[43] Yip HK, Lee MS, Li YC, Shao PL, Chiang JY, Sung PH, Yang CH and Chen KH. Dipeptidyl Peptidase-4 deficiency effectively protects the brain and neurological function in rodent after acute Hemorrhagic Stroke. Int J Biol Sci 2020; 16: 3116-3132.